

A 600°C Wireless and Passive Temperature Sensor Based on Langasite SAW-Resonators

Bert Wall¹, Richard Gruenwald¹, Matthias Klein¹, Gudrun Bruckner²

¹ Vectron International GmbH, Potsdamer Str. 18, D-14513 Teltow, Germany, wall@vectron.com

² CTR Carinthian Tech Research AG, Europastraße 4/1, Technologiepark Villach, A-9524 Villach/St. Magdalen, Austria

Abstract:

A wireless temperature sensor for the measurement of temperatures up to 600°C was developed. The passive sensor is based on SAW resonators on Langasite substrate. To support temperatures up to 600°C, new processes for front-end and back-end were developed and new material parameters for simulation of SAW devices on Langasite had to be determined. The results for the applied metallization system are discussed. Novel and reliable solutions in the field of assembly technology of a high-temperature surface mount package are presented.

Wired and wireless measurements will be shown. Harsh environment reliability data, e.g. temperature cycling between 50°C and 650°C, temperature storage at 600°C and temperature measurements up to 700°C will be demonstrated. The development of appropriate resonator designs and investigations made for definition of operating frequency range of sensors are covered. For wireless interrogation, an antenna optimised for high temperature operation at 433 MHz was developed.

Key words: temperature sensor, high-temperature, wireless interrogation, passive sensor, SAW sensor

Introduction

Accurate in-situ temperature measurement is a key requirement for energy-efficiency and process control in many physical and chemical processes requiring high-temperatures. Typical available methods for measuring high-temperatures around 600°C are based on resistance temperature detectors (RTDs), like PT1000, or thermal radiation measurement. Both approaches require either a direct hard-wired interconnection or a close visual contact. Therefore, the temperature measurement at critical locations such as rotating or reciprocating parts like turbine blades or engine pistons is complicated or impossible. In these types of applications, SAW-based passive wireless temperature sensing technology offers distinct advantages over these established measurement methods, including passive operation and wireless interrogation. This makes them well suited for rotating applications and for those applications where sensors are placed in regions difficult to reach, isolated locations or high voltage environments [1].

SAW-based temperature sensing can be realized by inducing a surface acoustic wave on a piezoelectric material, whereas the energy required for this is provided through wireless transmission. For resonant structures as described in this paper, the electric signal received by the SAW sensor is converted into acoustic energy and is stored within the resonator structure. When transmission is stopped, the stored energy continues to be backscattered as an electromagnetic signal, while the resonance

frequency of the SAW device, and therefore the frequency of the back-scattered signal, depends on the device's temperature. Such passive, wireless, SAW-based sensing systems have been described in many publications, e.g. [2, 3]. The measurement principle is described in figure 1.

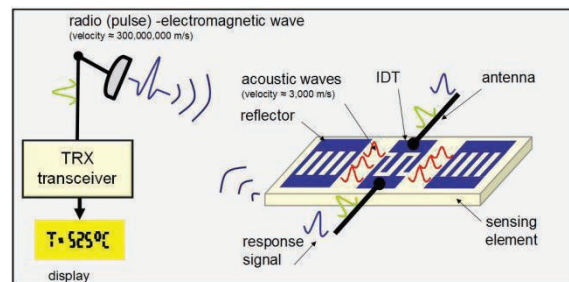


Fig. 1. Schematic drawing of a wireless temperature sensing system using SAW resonators.

Pushing the Temperature Limits

To realize SAW sensors operating up to 600°C, new wafer-level and assembly processes had to be developed. The most common piezoelectric crystals used for SAW devices, quartz, LiTaO₃ and LiNbO₃, were not applicable for this development. None of these is suitable for high-temperature sensors operating at 600°C. Quartz shows a phase transition from α - to β -quartz at 573°C, LiTaO₃ has a Curie temperature of 600°C...610°C and LiNbO₃ is affected by decomposition above 300°C [4].

Langasite (La₃Ga₅SiO₁₄ or LGS) was selected as high-temperature piezoelectric substrate material for

this project. It shows no phase transition up to its melting point of 1470°C, is available as 100 mm-wafers and can be processed applying common photolithography techniques. The use of LGS as piezoelectric crystal for SAW sensor devices has been reported extensively [5, 6].

High Temperature Stable Metallization System

For fabrication of SAW devices thin, temperature stable metal layers are required. Thin pure platinum layers show dewetting or agglomeration effects at a temperature of 600°C, therefore, a multi-layer stack consisting of Al/Al_xO_y/Pt was developed (patent pending). Applying high-temperature annealing steps, an Al/Al_xO_y surface layer is generated, covering the platinum and protecting it from dewetting. TEM (Transmission Electron Microscopy) and EDX (Energy Dispersive X-ray spectroscopy) analysis of the multi-layer stack are shown in figures 2 and 3 respectively.

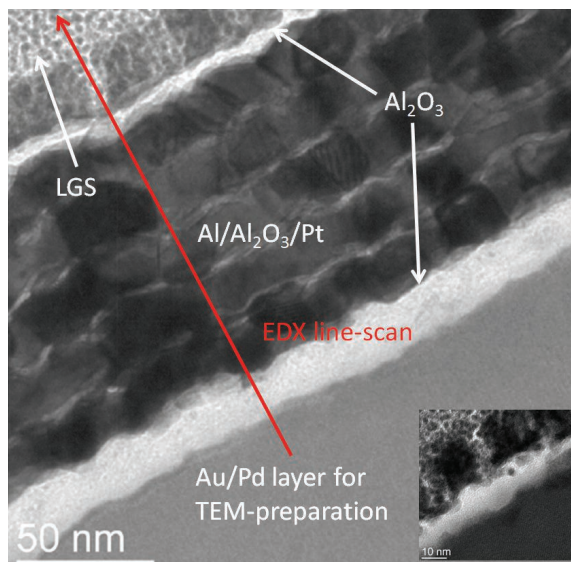


Fig. 2. TEM analysis of a high-temperature stable Al/Al_xO_y/Pt multi-layer stack, including five platinum layers, after annealing.

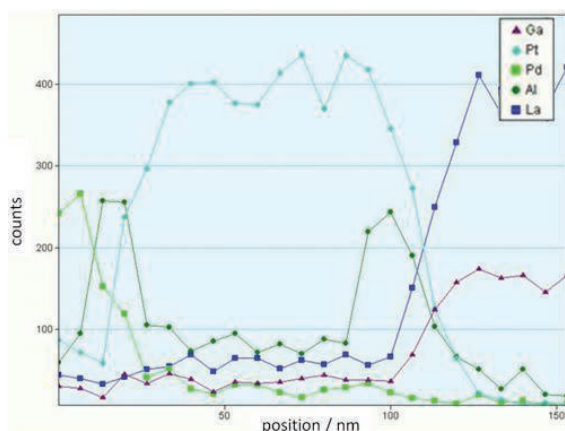


Fig. 3. EDX line-scan of Al/Al_xO_y/Pt multi-layer stack shown in figure 2.

Vertical grain boundaries within the Al/Al_xO_y/Pt metallization reflect deposition in layers. After high-temperature annealing, an influence of the horizontal

grain structure on the composition of the Langasite surface is visible (detail of figure 2)

Definition of Frequency Range for Wireless Interrogation

The operating band of the wireless interrogation system is centered at 433.92 MHz. This is a compromise between size of antennas for wireless interrogation and life time of SAW sensor elements at high-temperatures. An accelerated aging for increasing frequency of the surface acoustic wave was determined by measuring insertion attenuation of pass bands of harmonic delay lines. A measurement result of a harmonic delay line on Langasite of an early stage of the Al/Al_xO_y/Pt multi-layer stack is shown in figure 4. The structure is designed to have pass bands at 142 MHz, 420 MHz, 690 MHz and 967 MHz.

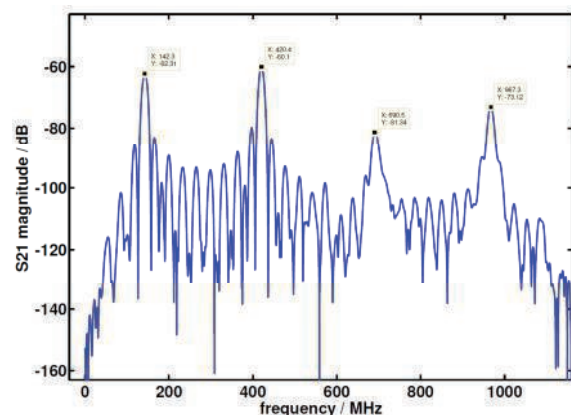


Fig. 4. Magnitude over frequency of a harmonic delay line with four pass bands.

If insertion loss of all pass bands is repeatedly measured over time during heat treatment at temperature levels of 260°C, 480°C and 650°C, significant differences between the four pass bands occur at 650°C. Almost no degradation is visible for the pass band at 142 MHz, only a limited degradation at 420 MHz, but a strong degradation at 690 MHz. For the 967 MHz pass band no signal can be detected after heating the devices to 650°C. Measurement results for two delay lines, with different delay times are shown in figure 5. Temperature over time is plotted as dark green solid line.

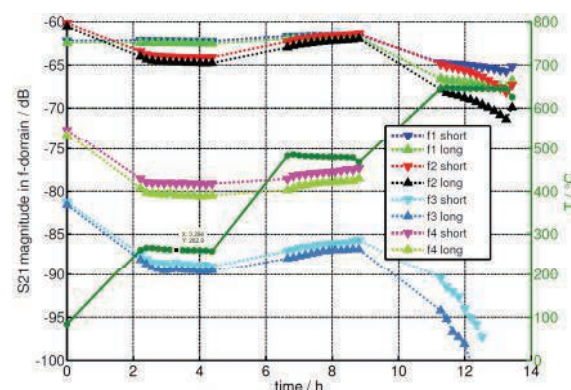


Fig. 5. Magnitude of two harmonic delay lines with different delay times (short and long) over time for four pass bands (f1...f4).

Determination of LGS Material Parameters

Calculations of temperature coefficient of frequency (TC_f) for Langasite with Pt-metallization or $Al/Al_xO_y/Pt$ multi-layer metallization based on previously available material parameters [7], [8], [9] showed significant deviations from our experimental results and results given in [10] for temperatures beyond 200°C. These calculations are mandatory to search for optimum crystal cuts for temperature sensors on Langasite. Therefore, a comprehensive study of material parameters of Langasite was completed [11]. Finally, the comparison between calculated and measured results reaches much better agreement for TC_f using the new material parameters (see "IFW" data in figure 6).

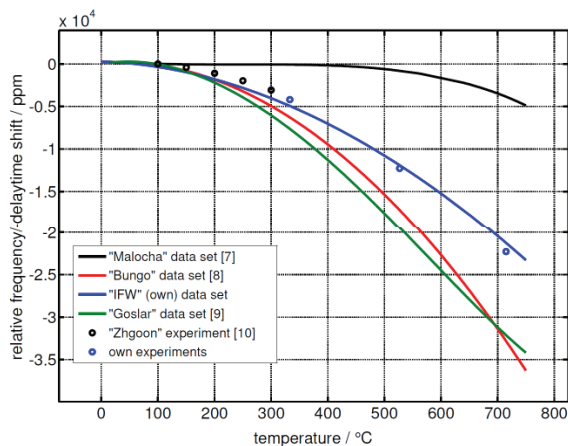


Fig. 6. Comparison of calculated temperature dependency of frequency or delay-time for SAW-devices on Langasite with Euler angles (0° , 138.5° , 26.6°) using different material parameter sets with measurements.

For simulation of resonators, the Coupling of Modes (COM) approach is used. For selected Langasite cuts with promising temperature coefficients COM-parameters were calculated successfully.

SAW-Resonator Design

One-port resonators on Langasite were designed and manufactured applying our $Al/Al_xO_y/Pt$ multi-layer stack for metallization.

The performance of different resonator designs was compared using equivalent circuit elements which were derived from measured one-port S-parameters. A five element equivalent circuit, which is shown in figure 5, was applied [12]. Using a five element equivalent circuit with R_0 , an equivalent circuit element for evaluation of ohmic losses within the structure of the one-port resonator is available.

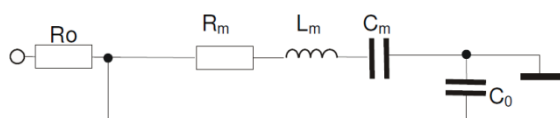


Fig. 7. Schematic of a five element equivalent circuit for one-port resonators.

Measurement results and equivalent circuit parameters for resonators on LGS with $Al/Al_xO_y/Pt$ multi-layer stack for metallization are shown in table 1. Noticeable is a relatively high ohmic

resistance within the structure. Further improvement of resonator Q by technology and design optimization is in progress.

Tab. 1: Measurement results and equivalent circuit parameters derived from 1-port S-parameters of high temperature resonators measured at room temperature

| | Qu | Ql | Rm [Ω] | Lm [μH] | Cm [fF] | Ro [Ohm] | Co [pF] | fs [MHz] |
|--------------------|-------|------|-----------|------------|------------|-------------|------------|-------------|
| | 2553 | 1377 | 45,65 | 54,10 | 2,42 | 12,87 | 2,72 | 439,566 |
| | 2847 | 1537 | 45,65 | 60,52 | 2,17 | 13,06 | 2,70 | 439,505 |
| | 3113 | 1652 | 43,82 | 63,69 | 2,06 | 12,69 | 2,72 | 439,586 |
| | 3018 | 1593 | 43,04 | 61,06 | 2,15 | 12,86 | 2,78 | 439,689 |
| | 3060 | 1577 | 40,35 | 58,86 | 2,23 | 12,77 | 2,79 | 439,568 |
| average | 2918 | 1547 | 43,70 | 59,65 | 2,20 | 12,85 | 2,74 | 439,583 |
| standard deviation | 203,2 | 92,8 | 1,96 | 3,18 | 0,122 | 0,121 | 0,035 | 0,060 |

High-Temperature Packaging

HTCC (High-Temperature Co-fired Ceramic) cavity packages for conventional operating temperatures were modified and tested for high-temperature application.

The most common materials for conductor lines and via structures within the Al_2O_3 multilayer package are the use of a tungsten or tungsten/molybdenum thick film structures. For standard wire- or flip-chip-bonded devices with conventional operating temperatures, a Ni/Au layer is deposited by electrolytic or electroless plating. Only a sub-micron gold layer is applied in order to simultaneously protect the nickel from oxidation and to prevent the back-side LGA (land grid array) pads used for the final soldering of the package on a PCB (printed circuit board) from the formation of brittle Sn/Au intermetallic phases. Besides Ni/Au, a second metal stack consisting of Pd/Au/Pt was evaluated. Both types of HTCC packages were then tested by thermal cycling between $+50^\circ\text{C}$ and $+650^\circ\text{C}$ (air-to-air, dwell time 30 min in normal atmosphere) for up to 100 cycles. Ni/Au as well as Pd/Au/Pt showed larger areas and spots of delamination after 100 thermal cycles.

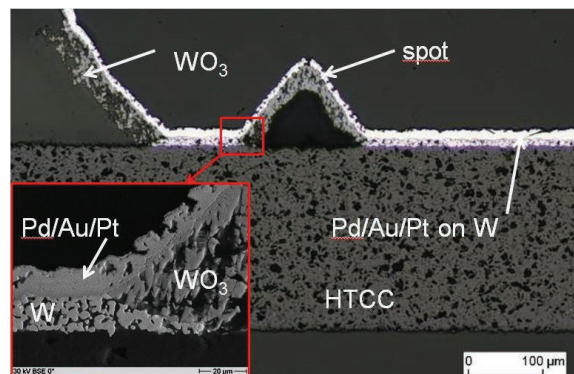


Fig. 8. SEM images of the cross section of a delamination spot after 50 temperature cycles ($+50^\circ\text{C}/+650^\circ\text{C}$ in air) of a HTCC package with W/Pt/Au/Pd metallization.

The SEM image in figure 8 depicts the degradation of the die-attach area of a tested $9 \times 7 \text{ mm}^2$ HTCC package with Pd/Au/Pt metallization. Analyses of the metallization on the die attach area clearly indicate

the formation of a tungsten oxide, which is assumed to be WO_3 , underneath the top layer metallization. The investigated metal layer stacks are obviously not able to fully protect the tungsten metallization from oxidation. To overcome these issues, we developed a robust, reliable and stable ceramic packaging technology for harsh and highest temperature environments which we call “eHTP” (extreme High-Temperature Package). It is a HTCC cavity package having a size of $5 \times 5 \text{ mm}^2$. Instead of tungsten, a platinum-based metallization was selected for interconnections, pads and vias. A cross section of the package is shown in figure 9 (A) and an overview of the package in 9 (B). This Pt/glass metallization was qualified to be compatible with soldering, wire-bonding as well as brazing interconnection technologies. This allows flexibility in performing either chip-on-board (COB) in combination with wire-bonding or flip-chip (FC)-bonding processes. Figure 9 (C) depicts, as an example, the cross section of a successfully thermo-sonic (TS) bonded platinum stud bump to the platinum metallization

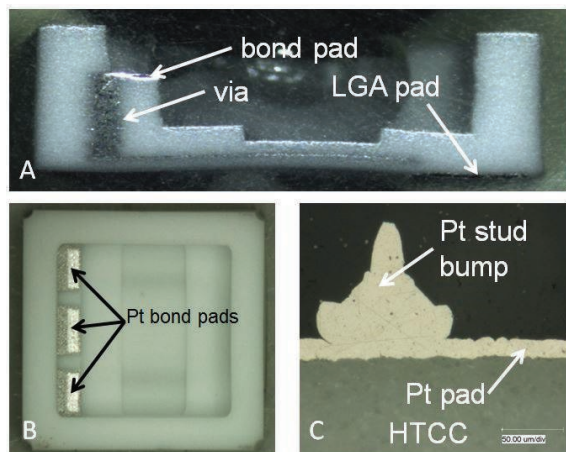


Fig. 9. Light microscopy images: cross section of the “eHTP” cavity package showing a bond pad on a pedestal and a back side LGA pad (A), the top view of the package (B) and a cross section of a Pt stud bump TS-bonded to a Pt pad (C).

An assembly method for SAW dies, resulting in a low mechanical stress on the chip, was chosen. The SAW die is split into two functional areas, an interconnect area for mechanical and electrical connection and an active micro-acoustic area (see figure 10).

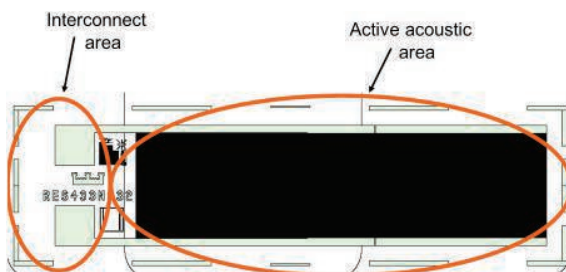


Fig. 10. Schematics of stress-reduced design for one-port resonators.

A high-temperature hermetic sealing process was developed to reliably seal the package and to guarantee an appropriate atmosphere inside the device (e.g. inert gas or vacuum). The crucial role of

the atmosphere inside packages used for high-temperature SAW devices is described in detail in [13]. To minimize the mechanical stress for a sealed package, the same type of ceramic as used for the cavity package was selected as lid material (see figure 11). More details about high temperature packaging and our “eHTP” solution are presented in [14].

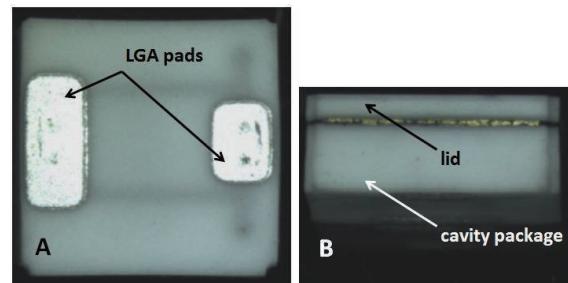


Fig. 11. Light microscopy images of a high temperature sensor applying the “eHTP” housing with the LGA pads on the back side (A) and after the hermetical sealing with a ceramic lid (side view, (B))

High-Temperature Antenna

For the use of the sensor in high-temperature environments coil as well as PIF (Planar Inverted F-shaped) antennas were designed and analysed (see figure 12).

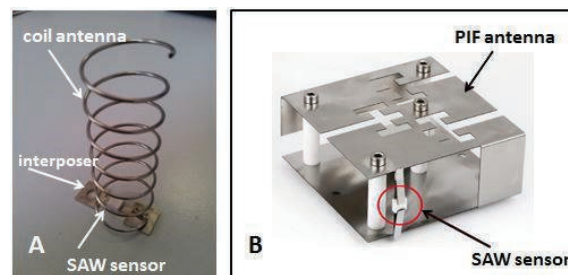


Fig. 12. Images of high-temperature SAW sensor solutions with “eHTP” housing connected to a coil antenna by brazing to metal interposers (A) and connected to a PIFA by clamping (B).

Although coil antennas are simple to manufacture and easy to trim in frequency, their bandwidth is smaller compared to PIFA. The more complex design of the PIFA allows reaching a fractional bandwidth of 10% with a relatively small form factor. The PIFA shown in figure 12 (B), with a centre frequency of 433 MHz, has a planar size of $65 \times 65 \text{ mm}^2$ and a mechanically robust design avoiding deformation at operating temperatures up to 600°C .

For electrical interconnection between the SAW sensor within our “eHTP” and antennas brazing and clamping has been analysed. Clamping of the sensor package between flexible steel plates is a fast and easy to use solution for wireless measurement of a higher number of sensor elements and antennas. The return loss of PIF-antennas brazed to a high temperature sensor element, as shown in figure 13, was measured wired using a network analyser. The sharp peak within the characteristic indicates the frequency of the high-temperature sensor’s resonance peak.

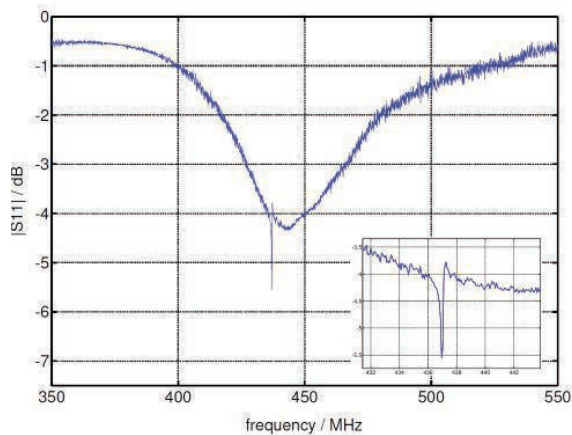


Fig. 13. Measured return loss of a temperature sensor module with PIF-antenna.

Reliability of the Temperature Sensor

Three different tests were performed analyzing the reliability of the high-temperature SAW sensor, covering thermal cycling, step-stress-test and long term high-temperature storage.

Thermal cycling: The test conditions are the same as applied for the test of the before mentioned HTCC metal layer system, i.e. temperature cycling between +50°C and +650°C, air-to-air, with a dwell time of 30 min in normal atmosphere. Most critical during this test is the hermeticity of the package. Nine sensor devices were tested for 75 cycles and measurements were performed after 25, 50 and 75 cycles. No relevant performance change of the devices was detected, indicating that a reliable interconnection between lid and cavity package was realized by the high-temperature hermetical sealing process.

The diagram in figure 14 depicts, for example, the conductance measured at room temperature for a single sensor before and after performing the thermal cycling test. Neither the quality factor of the sensors nor their resonance frequency shows any relevant degradation after thermal cycling test.

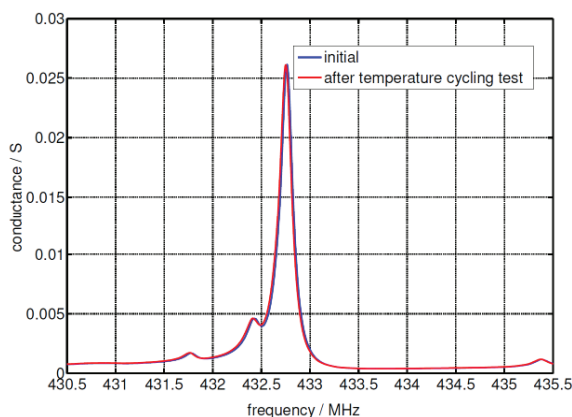


Fig. 14. Conductance at room temperature for a single sensor before and after performing the thermal cycling test.

Step-stress-test: Eight temperature sensors were measured in wired condition in a vacuum furnace. For a detailed description of the test equipment see [15]. The measurement started at 550°C, continued

at 600°C and was subsequently raised up to 700°C in steps of 20 K. The dwell time for each step was 46.5 h, resulting in a test duration of about two weeks.

All tested sensors passed the step-stress-test successfully. No relevant degradation was measured. The diagram in figure 15 depicts, for example, the results of the resonance frequency measurement of a single sensor.

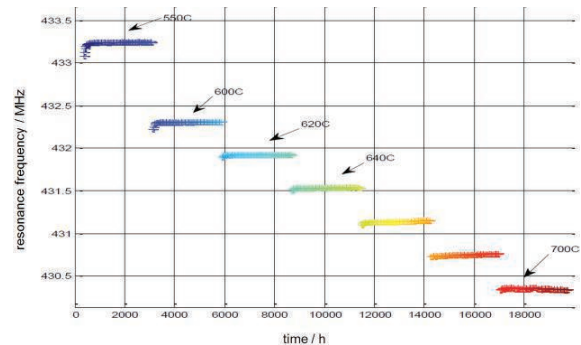


Fig. 15. Resonance frequency of a single high temperature resonator during step-stress-test.

Long term stability: Three eHTP devices, containing SAW dies with test structures, were stored at 600°C in normal atmosphere for 1000 h. Measurements before, during and after the temperature storage showed no degradation of the devices, thus indicating a stable technological solution.

Conclusions

A temperature sensor for wireless and passive measurement of temperatures up to 600°C was developed, which is based on SAW resonators on Langasite substrate. New solutions for front-end and back-end processes were developed, including a high temperature stable Al/Al_xO_y/Pt multi-layer metallization for the SAW die and a high temperature packaging solution called “eHTP”. New material parameters for simulation of SAW devices on Langasite were developed allowing design of SAW sensors with a predictable frequency over temperature characteristic for a wide temperature range.

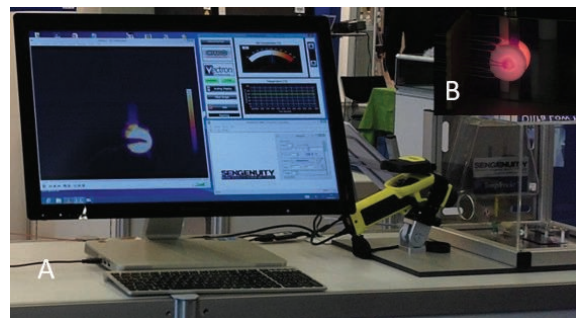


Fig. 16. Pictures of life presentation of wireless interrogation of high-temperature sensor at trade show SENSOR+TEST 2014 (A) and of a glowing miniaturized heater covering a high temperature sensor (B).

Wired measurement results were shown proving good stability for high-temperature operation including temperature storage at 600°C for 1000 h, a

temperature step-stress-test for temperatures between 550°C and 700°C and a temperature cycling test between 50°C and 650°C. For wireless interrogation, antennas optimized for high-temperature operation at 433 MHz were developed. In combination with standard wireless readers, a technology demonstrator showing the capability of wireless interrogation at temperatures up to 600°C was presented at SENSOR+TEST 2014 (see figure 16).

Acknowledgements

The authors would like to thank J. Bardong and S. Jaster for their support.

This work was performed co-funded within the R&D program COMET - Competence Centers for Excellent Technologies - by the Federal Ministries of Transport, Innovation and Technology (BMVIT) and Economics and Labour (BMWA), managed on their behalf by the Austrian Research Promotion Agency (FFG). Additional financial support by the Austrian Province of Carinthia is also gratefully acknowledged.

References

- [1] J. Andle, S. Sabah, D. Stevens, S. Jumani, M. Baier, B. Wall, T. Martens, R. Gruenwald, Temperature Monitoring System Using Passive Wireless Sensors for Switchgear and Power Grid Asset management, *T&D Asset Management Workshop, MNC-CIGRE/CIREC*, Malaysia, December 2010
- [2] F. Seifert, A. Pohl, R. Steindl, L. Reindl, M.J. Vellekoop, B. Jacoby, Wirelessly Interrogable Acoustic Sensors, *1999 Joint Meeting of the European Frequency and Time Forum and the IEEE International Frequency Control Symposium Proceedings*, 1013-1018 (1999), doi: 10.1109/FREQ.1999.841477
- [3] R. Fachberger, G. Bruckner, R. Hauser, L. Reindl, Wireless SAW based high-temperature measurement systems, *2006 IEEE International Frequency Control Symposium and Exposition Proceedings*, 358-367 (2006), doi: 10.1109/FREQ.2006.275412
- [4] J. Hornsteiner, E. Born, G. Fischerauer, E. Riha, Surface Acoustic Wave Sensors for High-Temperature Applications, *Proceedings of the 1998 IEEE International Frequency Control Symposium*, 615-620 (1998), doi: 10.1109/FREQ.1998.717964
- [5] B. Francois, D. Richter, H. Fritze, Z.J. Davis, C. Droit, B. Guichardaz, V. Petrini, G. Martin, J.M. Friedt, S. Ballandras, Wireless and Passive Sensors for High Temperature Measurements, *The Third International Conference on Sensor Device Technologies and Applications Proceedings*, 46-51 (2012)
- [6] M. Pereira da Cunha, R.J. Lad, T. Moonlight, G. Bernhardt, D.J. Frankel, High Temperature Stability of Langasite Surface Acoustic Wave Devices, *IEEE International Ultrasonics Symposium 2008 Proceedings*, 205-208 (2008), doi: 10.1109/ULTSYM.2008.0050
- [7] D.C. Malocha, M.P. da Cunha, E. Adler, R.C. Smythe, S. Frederick, M. Chou, R. Helmbold, Y.S. Zhou, Recent Measurements of Material Constants Versus Temperature for Langatate, Langanite and Langasite, *2000 IEEE/EIA International Frequency Control Symposium Proceedings*, 200-205 (2000), doi: 10.1109/FREQ.2000.887354
- [8] A. Bungo, C. Jian, K. Yamaguchi, Y. Sawada, S. Uda, Yu.P. Pisarevsky, Analysis of Surface Acoustic Wave Properties of the Rotated Y-cut Langasite Substrate, *Japanese Journal of Applied Physics*, vol. 38, 3239-3243 (1999), doi: 10.1143/JJAP.38.3239
- [9] M. Schulz, H. Fritze, Electromechanical Properties of Langasite Resonators at Elevated Temperatures, *Renewable Energy*, vol. 33, 336-341 (2008), doi: 10.1016/j.renene.2007.05.016
- [10] S. Sakharov, S. Kondratiev, A. Zabelin, N. Naumenko, A. Azarov, S. Zhgoon, A. Shvetsov, Theoretical and Experimental Investigation of Langasite as Material for Wireless High Temperature SAW Sensors, *2010 IEEE International Ultrasonics Symposium (IUS) Proceedings*, 535-538 (2010), doi: 10.1109/ULTSYM.2010.5935533
- [11] M. Weihnacht, A. Sotnikov, H. Schmidt, B. Wall, R. Gruenwald, Langasite: High Temperature Properties and SAW Simulations, *IEEE International Ultrasonics Symposium 2012 Proceedings*, 1549-1552 (2012), doi: 10.1109/ULTSYM.2012.0387
- [12] S. Klett, M. Binhack, W. Buff, M. Hamsch, R. Hoffman, Progress in Modeling of Sensor Function for Matched SAW Resonators, *IEEE International Ultrasonics Symposium 2002 Proceedings*, 471-474 (2002), doi: 10.1109/ULTSYM.2002.1193444
- [13] J. Bardong, G. Bruckner, M. Kraft, R. Fachberger, Influence of packaging atmospheres on the durability of high-temperature SAW sensors, *IEEE International Ultrasonics Symposium 2009 Proceedings*, 1680-1683, (2009), doi: 10.1109/ULTSYM.2009.5441557
- [14] M. Klein, B. Wall, R. Gruenwald, G. Bruckner, K. Ueki, Design, Assembly and Reliability of a Hermetic Package for a 600°C Wireless Temperature Sensor, will be presented in *65th Electronic Components and Technology Conference Proceedings* (2015)
- [15] J. Bardong, G. Bruckner, G. Franz, R. Fachberger, A. Erlacher, Characterisation setup of SAW Devices at High Temperatures and Ultra High Frequencies, *IEEE International Frequency Control Symposium Joint with the 22nd European Frequency and Time forum Proceedings*, 28-32, (2009), doi: 10.1109/FREQ.2009.5168136